Observation of frequency band gaps in a one-dimensional nanostructured magnonic crystal

Z. K. Wang,[1] V. L. Zhang,[1] H. S. Lim,[1] S. C. Ng,[1] M. H. Kuok,[1,a)] S. Jain,[2] and A. O. Adeyeye[2,b)]
[1]*Department of Physics, National University of Singapore, Singapore 117542, Singapore*
[2]*Department of Electrical and Computer Engineering, National University of Singapore, Singapore 117576, Singapore*

(Received 30 January 2009; accepted 8 February 2009; published online 27 February 2009)

We report the experimental observation of band gaps in a synthetic nanostructured magnonic crystal composed of two different magnetic materials. The sample, in the form of a one-dimensional periodic array comprising alternating Permalloy and cobalt nanostripes, has been fabricated using advanced lithographic techniques. Dispersion relations of spin waves in the magnonic crystal have been mapped by Brillouin spectroscopy. The center frequency and width of the band gaps observed are tunable by an applied magnetic field. Dispersion relations calculated based on the finite element method accord with the measured data. © *2009 American Institute of Physics*.
[DOI: 10.1063/1.3089839]

A photonic crystal is a periodic composite of materials with different dielectric constants. Analogously, a synthetic magnonic crystal can be considered as a periodic composite composed of different magnetic materials. While photonic crystals are a well known class of materials,[1] relatively little is known about magnonic ones. This is not surprising as magnonic crystals only started to attract considerable attention a few years ago.[2–7] Like photonic crystals, magnonic ones are expected to possess special and interesting properties arising from their frequency band gaps. Magnonic crystals form the basis of magnonics, an emerging field, which aims to control the generation and propagation of information-carrying spin waves by means analogous to the control of light in photonic crystals. Hence, synthetic magnonic crystals are expected to show great promise in wide-ranging applications such as in magnetoelectronic devices.[7] Puszkarski and Krawczyk[2,3] have theoretically established that the spin wave frequency band gaps, in a two-material magnonic crystal, depend on the spontaneous magnetization contrast and the exchange contrast. Previous experimental studies reported were performed on periodic structures composed of only one constituent magnetic material. They include micron-size shallow grooves etched on yttrium iron garnet (YIG) films,[8] two-dimensional array of micron-size holes etched on YIG films,[9,10] and one-dimensional (1D) arrays of micron-size metal stripes on YIG films.[11] In these investigations, highly attenuated frequency bands were observed using the microwave technique.

Spin waves in 1D periodic arrays of noncontacting Permalloy nanostripes were recently investigated by Gubbiotti *et al.*[12] and Kostylev *et al.*,[13] with the latter group reporting the observation of partial frequency band gaps. In these magnetic systems, no spin precession exists within the intervening air gaps in these arrays. As the edge-to-edge spacing between neighboring stripes in these systems was 55 nm, which is much larger than the exchange length (~5 nm) for Permalloy, the stripes are exchange decoupled. What both groups observed were collective spin waves arising from the closely spaced interacting stripes. Additionally, when the air gaps in these arrays are wider than the dipolar interaction range, the collective mode behavior ceases to exist and the observed modes are then confined within each individual isolated stripe.

Our work is motivated by the search for a synthetic nanostructured crystal, comprising more than one magnetic material, which exhibits a magnonic band gap within which no spin waves can propagate. It has been theoretically predicted that,[2,3] in general, the more contrasting the magnetic properties of the constituent materials of a magnonic crystal are, the wider would be its band gap, a property that can be exploited to facilitate detection of band gaps. For this reason, we chose cobalt and Permalloy as fabrication materials, as the saturation magnetization and exchange constant of the former are about twice those of the latter.

We have designed and fabricated a 1D magnonic crystal in the form of a periodic array comprising alternating contacting cobalt and Permalloy nanostripes. Unlike previously studied arrays of only one constituent magnetic material, spin precession exists throughout the entire length of our array, and thus spin waves can propagate across its entire length, regardless of the width of the stripes. Also, the choice of a second magnetic material in our type of magnonic crystals affords a greater versatility in the tailoring of the band structure (the gap width and/or center frequency). Brillouin light scattering (BLS), an excellent investigative tool for probing spin waves in nanostructures,[12–15] was employed to map the dispersion relations of the spin waves in this structure.

Most of the experimental work on periodic magnetic structures reported to date are based on magnetostatically coupled 1D nanowires of the same magnetic material[12,13] or modulated YIG films.[8] Our structure was fabricated on oxidized Si(001) substrate using high-resolution multilevel electron beam lithography, deposition, and lift-off processes. The first nanostripe array was defined on polymethyl methacrylate (PMMA) resist. This was followed by electron beam deposition and lift-off of a 30-nm-thick $Ni_{80}Fe_{20}$ (Py) film.

a)Electronic mail: phykmh@nus.edu.sg.
b)Electronic mail: eleaao@nus.edu.sg.

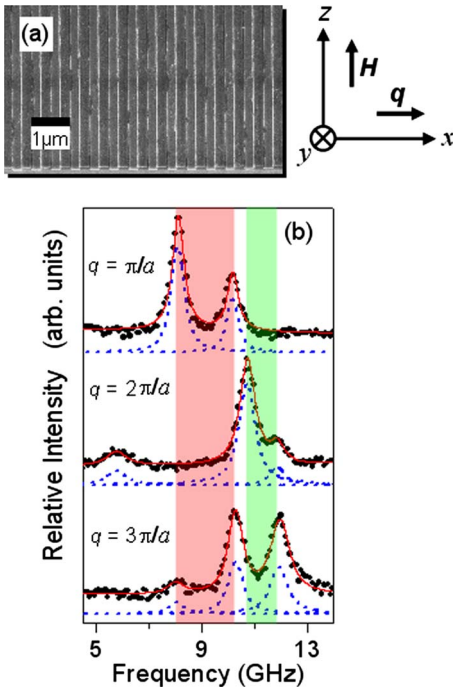

FIG. 1. (Color online) (a) SEM image of a magnonic crystal in the form of a 1D periodic array of 30-nm-thick Permalloy and cobalt nanostripes, each of width 250 nm. Coordinate system showing directions of applied magnetic field $\boldsymbol{H}$ and magnon wave vector $\boldsymbol{q}$. (b) Brillouin spectra ($H=0$) recorded at various BZ boundaries. The shaded regions represent frequency band gaps. All spectra were fitted with Lorentzian functions (dashed curves), and the resultant fitted spectra are shown as solid curves.

For the fabrication of the second nanostripe array, another layer of PMMA resist was deposited. High-resolution electron beam lithography with precise alignment was then used to define the position of the second nanostripe array. Subsequently, a 30-nm-thick cobalt film was deposited. The stripes of the resulting nanostructured arrays are very well-aligned as evidenced by the representative scanning electron microscope image shown in Fig. 1(a). As adjacent stripes are in direct physical contact, they are exchange coupled together.

A crystal with a period (lattice constant) $a=500$ nm and stripe width of 250 nm was fabricated. All stripes have a length of 100 microns and a thickness of 30 nm, and the length of the array is 100 microns. For brevity, the sample will be referred to as 250 nm Co/250 nm Py. The periodicity of the crystal was chosen so that, for the experimentally accessible spin wave vectors, the dispersion spectrum can be measured up to the fourth Brillouin zone (BZ).

BLS measurements were performed in the 180°-backscattering geometry and in *p-s* polarization using a 6-pass tandem Fabry–Pérot interferometer, and the $\lambda=514.5$ nm radiation of an argon-ion laser for excitation. Prior to the start of an experiment, each sample was saturated in a 1 T field directed parallel to the *z*-axis [see Fig. 1(a)]. In magnetic field dependence experiments, the applied static field $\boldsymbol{H}$ was generated with a computer-controlled electromagnet. By varying the laser light incidence angle θ, the dispersion relations were mapped across BZs, i.e., over the range of the magnon wave vector $q(=4\pi \sin\theta/\lambda)$ from zero up to as high as $4\pi/a$.

Representative Brillouin spectra ($H=0$) of the sample, recorded at various BZ boundaries, are presented in Fig. 1(b). The frequencies of the three observed peaks, obtained from a fit with Lorentzian functions, were plotted as a function of magnon wave vector and displayed in Fig. 2. The periodic character of the three dispersion branches, measured up to the fourth BZ, is evident from the figure. Another notable feature of the dispersion spectrum is the two direct energy band gaps. The widths of the first and second band gaps were measured to be 2.1 and 1.2 GHz respectively.

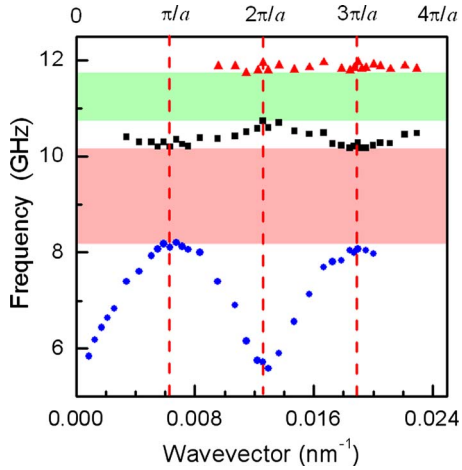

FIG. 2. (Color online) Measured dispersion relations ($H=0$), featuring band gap structures, of spin waves in the 250 nm Co/250 nm Py magnonic crystal with lattice constant $a=500$ nm. Experimental data are denoted by symbols. The first and second frequency band gaps are represented by shaded bands. The BZ boundaries ($q=n\pi/a$) are represented by dashed lines.

The behavior of the magnonic band structures under a magnetic field was also investigated. The band structure of the 250 nm Co/250 nm Py sample measured at $H=0.2$ T$/\mu_0$ is presented in Fig. 3(a). Figure 3 reveals that under the application of a magnetic field, the entire band structure is shifted up in frequency, while both the band gaps become narrower. In the case of the first gap, its center frequency increases from 9.4 to 32.6 GHz when the field is raised from $H=0$ to 0.7 T$/\mu_0$ [see Fig. 3(c)]. In contrast, its width decreases from 2.1 to 0.6 GHz [see Fig. 3(d)].

Calculations of the dispersion relation were carried out as follows: The magnetic stripes are treated as being infinitely long in the *z*-direction [see Fig. 1(a)]. Linearization of the Landau–Lifshitz equation gives[16]

$$i\Omega m_x(\boldsymbol{r}) + (\nabla \cdot Q\nabla)m_y(\boldsymbol{r}) - m_y(\boldsymbol{r}) - \frac{M_s}{H}\frac{\partial \Psi(\boldsymbol{r})}{\partial y} = 0, \quad (1)$$

and

$$-(\nabla \cdot Q\nabla)m_x(\boldsymbol{r}) + m_x(\boldsymbol{r}) + i\Omega m_y(\boldsymbol{r}) + \frac{M_s}{H}\frac{\partial \Psi(\boldsymbol{r})}{\partial x} = 0, \quad (2)$$

where $\Omega=\omega/(\gamma\mu_0 H)$, $Q=2A/(M_s\mu_0 H)$, A is the exchange constant, M_s the saturation magnetization, γ the gyromagnetic ratio, H the applied magnetic field, m_x and m_y the components of the dynamic magnetization $\boldsymbol{m}$, ω the spin wave angular frequency, and $\boldsymbol{r}$ the three-dimensional position vector. The magnetic potential $\Psi(\boldsymbol{r})$, within the magnetic materials, is given by

$$\nabla^2\Psi(\boldsymbol{r}) = \frac{\partial m_x(\boldsymbol{r})}{\partial x} + \frac{\partial m_y(\boldsymbol{r})}{\partial y}, \quad (3)$$

while outside the materials, it satisfies the Laplace equation.

For simplicity, the surface anisotropy and interface exchange coupling are neglected so that, at the interface between the cobalt and Permalloy stripes, the exchange bound-

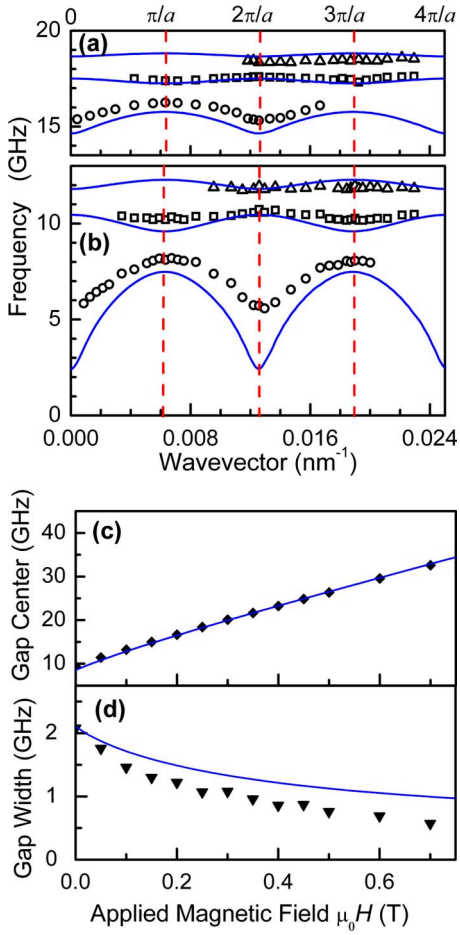

FIG. 3. (Color online) Measured and calculated magnonic band structures of 250 nm Co/250 nm Py magnonic crystal in (a) $H=0.2$ T$/\mu_0$ and (b) $H=0$. The BZ boundaries, corresponding to $a=500$ nm, are marked by dashed lines. Dependence of (c) center frequency, and (d) width of the first band gap on applied magnetic field. Measured and calculated data are represented by symbols and curves respectively.

ary conditions require the continuity of the magnetization $\boldsymbol{m}$ and $(A/M_s)(\partial \boldsymbol{m}/\partial x)$.[17] Magnetostatic boundary conditions also require that $\Psi(\boldsymbol{r})$ and the normal component of the magnetic induction be continuous across interfaces between two media. As the propagating spin waves are modulated by the periodicity of the magnonic crystal, the Bloch–Floquet theorem can be applied to give $\boldsymbol{m}(x+a)=\boldsymbol{m}(x)\exp(iqa)$. Thus, only a unit cell of the repeating structure needs to be considered and with periodic boundary conditions imposed. Finally, Eqs. (1)–(3), with the above-stated interface and surface boundary conditions, are numerically solved using the finite element method (FLEXPDE package)[18] to yield the dispersion relation $\omega(q)$.

Separate BLS measurements were carried out on the reference 30-nm-thick cobalt and Permalloy films. Least-squares fitting to the measured data yielded the magnetic parameters $M_s=1.15\times10^6$ A/m, $A=2.88\times10^{-11}$ J/m, and $\gamma=198.8$ GHz/T for cobalt, and $M_s=6.58\times10^5$ A/m, $A=1.11\times10^{-11}$ J/m, and $\gamma=190.5$ GHz/T for Permalloy. These parameters were then used to evaluate the dispersion relations. The calculated spin wave dispersion spectra for $H=0.2$ T$/\mu_0$ and 0, are presented in Figs. 3(a) and 3(b), while the calculated magnetic field dependence of the gap parameters is presented in Figs. 3(c) and 3(d). Figure 3 reveals that calculations accord fairly well with experimental data, showing that the theoretical treatment captures the magnetic field dependent features of the Brillouin data. The quantitative discrepancy is partly attributed to the nonconsideration of the interface/surface anisotropy and the interface exchange coupling between adjacent contacting stripes.

In summary, we have designed and fabricated a magnonic crystal in the form of 1D periodic arrays of alternating contacting stripes of different magnetic materials (cobalt and Permalloy), and have mapped its complete dispersion relations. The experimental establishment of the existence of magnonic band gaps in such a structure is expected to stimulate further development of the theory and applications of magnonics, an emerging field which holds enormous potential. Additionally, our magnonic crystal was found to exhibit band gap tunability, an important property which could find applications in the control of the generation and propagation of information-carrying spin waves in devices based on these crystals. Filters and waveguides, in which spin waves are generated by microwave techniques for use in microwave communication systems, are possible examples of such devices. The observed Brillouin peaks are generally sharp, suggesting that the spin waves are weakly attenuated as they propagate through the magnonic crystal. Hence, any loss in devices based on this structure is expected to be small.

Grant funding from the Ministry of Education Singapore, under research Project Nos. R144-000-239-112 and R144-000-141-112, is gratefully acknowledged.

[1] J. D. Joannopoulos, P. R. Villeneuve, and S. Fan, Nature (London) **386**, 143 (1997).
[2] M. Krawczyk and H. Puszkarski, Phys. Rev. B **77**, 054437 (2008).
[3] H. Puszkarski and M. Krawczyk, Solid State Phenom. **94**, 125 (2003).
[4] V. V. Kruglyak and R. J. Hicken, J. Magn. Magn. Mater. **306**, 191 (2006).
[5] S. A. Nikitov, C. S. Tsai, Y. V. Gulyaev, Y. A. Filimonov, S. L. Vysotskii, and P. Tailhades, Mater. Res. Soc. Symp. Proc. **834**, 87 (2005).
[6] S. A. Nikitov, P. Tailhades, and C. S. Tsai, J. Magn. Magn. Mater. **236**, 320 (2001).
[7] V. V. Kruglyak and A. N. Kuchko, Physica B **339**, 130 (2003).
[8] A. V. Chumak, A. A. Serga, B. Hillebrands, and M. P. Kostylev, Appl. Phys. Lett. **93**, 022508 (2008).
[9] Y. V. Gulyaev, S. A. Nikitov, L. V. Zhivotovskii, A. A. Klimov, P. Tailhades, L. Presmanes, C. Bonningue, C. S. Tsai, S. L. Vysotskii, and Y. A. Filimonov, J. Exp. Theor. Phys. **77**, 567 (2003).
[10] S. L. Vysotskii, S. A. Nikitov, and Y. A. Filimonov, J. Exp. Theor. Phys. **101**, 547 (2005).
[11] M. E. Dokukin, K. Togo, and M. Inoue, J. Magn. Soc. Jpn. **32**, 103 (2008).
[12] G. Gubbiotti, S. Tacchi, G. Carlotti, N. Singh, S. Goolaup, A. O. Adeyeye, and M. Kostylev, Appl. Phys. Lett. **90**, 092503 (2007).
[13] M. Kostylev, P. Schrader, R. L. Stamps, G. Gubbiotti, G. Carlotti, A. O. Adeyeye, S. Goolaup, and N. Singh, Appl. Phys. Lett. **92**, 132504 (2008).
[14] Z. K. Wang, M. H. Kuok, S. C. Ng, D. J. Lockwood, M. G. Cottam, K. Nielsch, R. B. Wehrspohn, and U. Gosele, Phys. Rev. Lett. **89**, 027201 (2002).
[15] Z. K. Wang, H. S. Lim, H. Y. Liu, S. C. Ng, M. H. Kuok, L. L. Tay, D. J. Lockwood, M. G. Cottam, K. L. Hobbs, P. R. Larson, J. C. Keay, G. D. Lian, and M. B. Johnson, Phys. Rev. Lett. **94**, 137208 (2005).
[16] J. O. Vasseur, L. Dobrzynski, B. Djafari-Rouhani, and H. Puszkarski, Phys. Rev. B **54**, 1043 (1996).
[17] V. V. Kruglyak, R. J. Hicken, A. N. Kuchko, and V. Y. Gorobets, J. Appl. Phys. **98**, 014304 (2005).
[18] FLEXPDE, finite element software, PDESolutions Inc.